

Widely tunable in the mid-IR BaGa₄Se₇ optical parametric oscillator pumped at 1064 nm

NADEZHDA Y. KOSTYUKOVA,^{1,2,3} ANDREY A. BOYKO,^{1,2,3} VALERIY BADIKOV,⁴ DMITRII BADIKOV,⁴
 GALINA SHEVYRDYAEVA,⁴ VLADIMIR PANYUTIN,¹ GEORGI M. MARCHEV,¹
 DMITRY B. KOLKER,³ AND VALENTIN PETROV^{1,*}

¹Max-Born-Institute for Nonlinear Optics and Ultrafast Spectroscopy, 2A Max-Born-Str., D-12489 Berlin, Germany

²Special Technologies, Ltd., 1/3 Zelfjonaja gorka Str., 630060 Novosibirsk, Russia

³Research Laboratory of Quantum Optics Technology, Novosibirsk State University, 2 Pirogova Str., 630090 Novosibirsk, Russia

⁴High Technologies Laboratory, Kuban State University, 149 Stavropolskaya Str., 350040 Krasnodar, Russia

*Corresponding author: petrov@mbi-berlin.de

Received 3 June 2016; revised 9 July 2016; accepted 11 July 2016; posted 11 July 2016 (Doc. ID 267622); published 1 August 2016

A BaGa₄Se₇ nanosecond optical parametric oscillator (OPO) shows extremely wide idler tunability in the mid-IR (2.7–17 μm) under 1.064 μm pumping. The ~10 ns pulses at ~7.2 μm have an energy of 3.7 mJ at 10 Hz. The pump-to-idler conversion efficiency for this wavelength reaches 5.9% with a slope of 6.5% corresponding to a quantum conversion efficiency or pump depletion of 40%. © 2016 Optical Society of America

OCIS codes: (190.4970) Parametric oscillators and amplifiers; (190.4400) Nonlinear optics, materials.

<http://dx.doi.org/10.1364/OL.41.003667>

There are only a few non-oxide nonlinear optical crystals that can be used for frequency downconversion of high-power solid-state laser systems operating near 1 μm (e.g., Nd:YAG at 1.064 μm) to the mid-IR (3–30 μm) and, in particular, beyond ~5 μm, the upper wavelength cutoff limit of oxide-based materials [1]. From the non-oxide crystals that are free of two-photon absorption (TPA), i.e., exhibit a bandgap corresponding to <0.532 μm, only very few have been applied in short (ns) pulse optical parametric oscillators (OPOs) pumped at 1.064 μm [2]. Initial experiments were performed with proustite (Ag₃AsS₃), a material that has been subsequently substituted by the chalcopyrite type AgGaS₂ (AGS) which is the only commercially available such crystal. AGS has generated so far the longest idler wavelengths for 1 μm pumped OPOs, 11.3 μm [3], while the highest output energies beyond 5 μm, 3 mJ at 6.3 μm, were achieved with the related defect chalcopyrite HgGa₂S₄ (HGS) [4] which is extremely difficult to grow in large sizes. Other nonlinear crystals for which such OPO operation has been reported [2] include the solid solution defect chalcopyrite Cd_xHg_{1-x}Ga₂S₄, for which the composition control presents a major problem, the chalcopyrite type CdSiP₂ (CSP), which shows the highest nonlinearity and figure of merit, but low damage threshold and an upper transparency limit of only ~6.5 μm, and the wurtzite type LiInSe₂ (LISE)

and LiGaS₂ (LGS), which exhibit modest nonlinearity, comparable or inferior to that of AGS [1].

Recently, we added a newly developed chalcogenide crystal, BaGa₄S₇ (BGS) with an orthorhombic *mm2* structure, to the short list of non-centrosymmetric nonlinear crystals of this kind that can be pumped at 1.064 μm [5]. It showed a tunability range from ~5.5 to 7.3 μm with a maximum energy of ~0.5 mJ at ~6.2 μm. Its selenide counterpart, BaGa₄Se₇ (BGSe), is expected to exhibit much higher nonlinearity [6]. BGSe is also biaxial, but monoclinic, i.e., it offers much more phase-matching options [6,7]. It exhibits a transparency extending from 0.776 to 14.72 μm at the 0.3 cm⁻¹ absorption level; however, the bandgap value, 2.64 eV, corresponds to 0.469 μm, i.e., no TPA is expected at 1.064 μm. Figure 1 shows a typical transmission spectrum of one of the BGSe samples used in this Letter (the sample itself is shown as an inset). Larger bandgap normally leads to higher damage threshold. Although we find the ~2.8 J/cm² specified in [8] for 5 ns pulses at 1.064 μm and 1 Hz exaggerated, our own estimation with 14 ns pulses at 100 Hz, gave a reasonably high value of 1.4 J/cm² leading to a peak on-axis intensity damage threshold

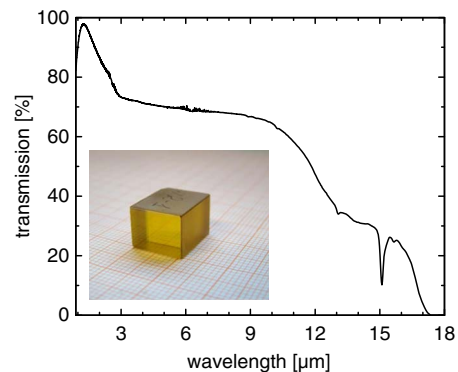


Fig. 1. Unpolarized transmission of the AR-coated sample BGSe-II; the inset shows a photograph of this sample.

of 100 MW/cm². The difference is mainly attributed to the unrealistically small OPO beam size used in [8], which was roughly 10 times larger in our own measurement with *z*-cut BGSe. The specified intensity value is the highest damage threshold compared to all non-oxide nonlinear crystals previously used in 1.064 μm pumped OPOs, except for the low-nonlinearity LGS and BGS which exhibit yet larger bandgaps.

More recently, very efficient optical parametric amplification was reported with ultrashort (30 ps) pump pulses at 1.064 μm and 10 Hz, achieving an idler tunability up to 11 μm with BGSe [9,10]. A BGSe OPO was also reported, but pumped at 2.091 μm [11], where the damage threshold is higher. Nevertheless, this typical 3–5 μm OPO essentially did not show tunability above the ~5 μm oxide crystal limit. Here we demonstrate, for the first time to the best of our knowledge, optical parametric oscillation in the mid-IR based on BGSe pumped at 1.064 μm. We report record long idler wavelengths (17 μm) for BGSe, achieving the highest conversion efficiency and the highest output idler energy above 5 μm (oxide materials limit) for any OPO pumped at 1.064 μm.

From the preliminary (unpublished) results on second-harmonic generation (SHG) and some partially resolved components of the second-order susceptibility tensor reported in [12], we decided to investigate two active elements made of BGSe. BGSe-I was a sample cut at $\theta = 46^\circ$ for ee-o positive type-I interaction in the *x*–*z* plane. Its dimensions were 10.33 mm (along *y*-axis) × 11.95 mm × 14.57 mm (length). The second sample BGSe-II was cut at $\theta = 33.5^\circ$ for oe-o positive type-II interaction in the *y*–*z* plane. This sample was slightly shorter, with dimensions of 9.22 mm (along *x*-axis) × 11.32 mm × 13.56 mm (length) mm. Both samples were AR coated for increased transmission at the signal wave which also resulted in a good transmission for the pump at 1.064 μm; see Fig. 1.

According to the monoclinic class *m* symmetry, the corresponding expressions for the effective nonlinearity of BGSe read [13]

$$d_{\text{eff}}(x-z) = d_{16} \cos^2 \theta + d_{23} \sin^2 \theta \quad (1)$$

in the *x*–*z* plane and

$$d_{\text{eff}}(y-z) = \pm d_{16} \cos \theta - d_{15} \sin \theta \quad (2)$$

in the *y*–*z* plane. In contrast to [7], we defined in Eqs. (1) and (2) the tensor components directly in the orthogonal dielectric frame *xyz*. We remind that under Kleinman symmetry $d_{16} = d_{21}$, $d_{23} = d_{34}$, and $d_{15} = d_{31}$. The dielectric frame is defined as usual from the refractive index relation $n_x < n_y < n_z$ and, for BGSe, the monoclinic *b*-axis coincides with the dielectric *x*-axis [7]. Unfortunately, the information on the components of the second-order susceptibility tensor is rather limited [12,14]. From the evaluated non-diagonal nonlinear coefficients, d_{23} is the largest, and d_{15} is negligible compared to it. The lack of information on d_{16} motivated us to study the two cases. Note that there exists also a third phase-matching possibility for such downconversion to the mid-IR: oe-o interaction in the *x*–*z* plane; however, $d_{\text{eff}} = -d_{24} \sin \theta$ for this case ($d_{24} = d_{32}$) and, from both [12] and [14], it follows that the efficiency of this process will be low. The sign \pm in Eq. (2) corresponds to different octants [13]. The actual octant is unknown for the available sample, but this additional degree of freedom cannot be utilized anyway, as long as the relative sign of d_{16} , both in Eqs. (2) and (1), is also unknown. Theoretical

calculations in [6] yield an opposite sign of d_{16} and d_{23} , and about a four times smaller value of d_{16} . However, the same model [6] results in contradiction with two of the measured nonlinear coefficients [12,14] and leads to incorrect predictions for the relation among the refractive indices.

The singly resonant OPO was set up with a standard linear cavity consisting of a flat input-output coupler (IOC) and a flat Au total rear reflector which ensures recycling of the pump and a double pass for the nonresonant idler prior to its extraction through the IOC, the same as the one shown in [5]. Pumping via a 45° ZnSe bending mirror that was highly transmitting for the signal and idler ensured separation of the input and output waves. Since the IOC was highly transmitting for the pump and idler and highly reflecting for the signal, the output consisted basically of the idler, which was characterized behind the bending pump mirror, suppressing any leakage from the pump and signal waves by suitable Ge cut-off filters.

The pump source was the same diode-pumped Nd:YAG master oscillator power amplifier system used in [5]. At 100 Hz, this system provided pulses of 8 ns duration with an energy of up to 250 mJ [5]. The output beam was passed through an attenuator (half-wave plate and polarizer) and a vacuum diamond pinhole and then down-collimated by a lens telescope to a Gaussian diameter of 5 mm in the position of the OPO. The spectral bandwidth of the pump beam was ~30 GHz (1 cm⁻¹) and $M^2 \sim 2$.

In this Letter, we decided to focus on the energetic performance of BGSe in the OPO and reduced the repetition rate of the pump laser by means of an external shutter to 10 Hz. The main reason for this was the damage limit we observed for all the available metallic total reflectors in terms of intensity when operating this system at 100 Hz [5]. Thus, all the following results apply for a repetition rate of 10 Hz.

Figure 2 shows the input–output OPO characteristics obtained at normal incidence for a short (24 mm) and slightly longer (32 mm) cavity. The antireflection (AR)-coated CaF₂ IOC shows no substrate absorption at the actual idler wavelengths, and the transmission is around 85% (6.3 μm). Its reflectivity measured at the signal wavelength (1.28 μm) is 73%. The pump energy given is the one incident on the BGSe crystals, while the idler energy is the one behind the IOC. The results with the 24 mm cavity in Fig. 2 and, in particular, the 3.7 mJ idler output at 7.2 μm, present the highest energy achieved in the mid-IR above 5 μm with a 1 μm pumped OPO [1,2]. With BGSe-II, a maximum energy of 4.7 mJ is obtained

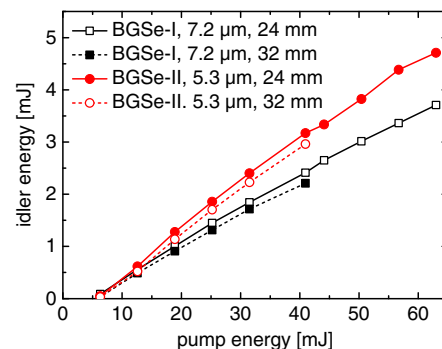


Fig. 2. Input–output characteristics of the BGSe OPO at normal incidence for a cavity length of 24 and 32 mm.

at 5.3 μm . This energy is much higher than the maximum output achieved at the longest idler wavelength of 5.19 μm (estimated to be <1.4 mJ from the total output presented in Fig. 2 in [11]) reported for the 2.091 μm pumped BGSe OPO.

The threshold is around 6 mJ for both BGSe crystals. The maximum pump level applied (63 mJ) corresponds to an axial fluence of 0.64 J/cm² or a peak on-axis intensity of 80 MW/cm², still below the damage threshold. However, pump depletion also helps to avoid damage to the BGSe samples in this highly efficient OPO. Assuming the same number of signal photons generated, the pump depletion is 40% for BGSe-I and 37% for BGSe-II, almost three times higher than the total conversion efficiency reported in [11] near degeneracy. At maximum pump level, the corresponding pump-to-idler energy conversion efficiencies are 5.9% and 7.5%, and the slope efficiencies are 6.5% and 8.3%. These slopes are only slightly lower compared to the initial part of the curves, i.e., the saturation is not strong. From the performance of BGSe-I and Eq. (1), one can conclude that the nonlinear coefficients d_{16} and d_{23} must have the same sign, contrary to the theoretical predictions in [6]. On the other hand, the performance of BGSe-II with Eq. (2) leads to the conclusion that d_{16} is substantially larger than d_{15} , i.e., it must be comparable in magnitude to d_{23} .

Under similar conditions, the performance of BGSe-I in terms of idler energy (3.7 mJ) was superior to that of HGS [4] also because it was obtained at a longer idler wavelength (7.2 against 6.3 μm), i.e., at decreasing parametric gain. Compared to the HGS OPO [4], the pump depletion achieved with BGSe-I is more than three times higher, the pump-to-idler efficiency is almost three times higher, and the slope efficiency is two times higher. While the roughly two times lower (in terms of pump fluence and intensity) threshold in this Letter compared to [4] can be explained by the shorter cavity length, shortening of the HGS OPO cavity resulted in lower slope efficiencies and no improvement in the pump-to-idler conversion efficiency at the maximum applied pump level [4]. Thus, it is difficult to explain the higher conversion efficiencies achieved in this Letter in comparison to HGS which exhibits the second highest figure of merit to CSP [1]. From comparison of the OPO performance, it is impossible to conclude that d_{eff} of BGSe is higher than that of HGS (related to the unknown magnitude of d_{16}). Another possibility here is the imperfect quality and increasing losses (including nonlinear) at higher pump levels in HGS when it comes to large optical elements (note that the nonlinear coefficients are measured with relatively small samples). Thus, the quality of the present BGSe samples seems to be excellent. Note that for HGS, at the maximum pump levels applied in [4] (very similar to this Letter in terms of fluence and intensity), the formation of scattering centers in the bulk was observed.

Tuning was studied by tilting the crystals in a lengthened cavity (32 mm). The AR-coated wedged ZnSe IOC employed for these measurements shows high transmission for the idler in a narrow spectral range for which it was optimized (95% at 6.3 μm). This transmission drops at longer wavelengths due to reflection losses (to $61 \pm 10\%$ between 7.5 and 17 μm) and at shorter wavelengths, from 72% at 4.7 μm to 37% at 2.7 μm . Its reflectivity for the signal is relatively flat, with 79% measured at 1.28 μm . The cavity lengthening itself

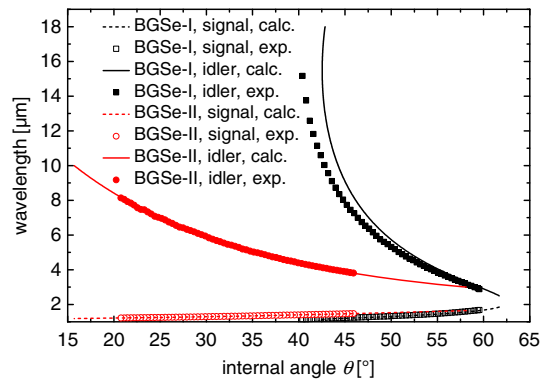


Fig. 3. Angle tuning of the OPO with BGSe-I and BGSe-II versus an internal phase-matching angle: symbols (experimental data) and curves (calculated with Sellmeier expressions from [15]).

had only a minor effect on the conversion efficiencies, as can be concluded from Fig. 2.

The experimental data for BGSe-II in Fig. 3 are in excellent agreement with calculations based on the Sellmeier equations presented in [15]. For BGSe-I, deviations exceeding 1° are seen, especially above 11 μm where the Sellmeier equations in [15] were not fitted.

The idler tuning range in Fig. 4 extends from 2.7 to 17 μm for BGSe-I and from 3.6 to 9.6 μm for BGSe-II. This result presents the longest wavelength ever achieved with a 1 μm pumped OPO [2,3]. In OPOs, the upper tuning limit is determined by the transparency and the decreasing parametric gain away from degeneracy. While the upper transparency limit of non-oxide crystals normally increases from phosphides via sulfides to selenides, BGSe is not the first selenide pumped at 1.064 μm [1,2]. LISe also exhibits a large bandgap; however, in this group of compounds, there is deviation from the above rule because the phonons that determine the mid-IR transparency limit are related to different types of vibrations, and LISe shows an upper limit similar to its sulfur counterpart. In addition, the nonlinearity of LISe is inferior to that of BGSe. Having extended transparency compared to BGS, BGSe delivered also much wider OPO tunability compared to its sulfur counterpart [5].

The wavelength dependence of the output energy is shown in Fig. 4. It is difficult to conclude from these results something about the magnitude and sign of d_{16} in Eqs. (1) and (2) because few other factors come into play. Typical enhancement is

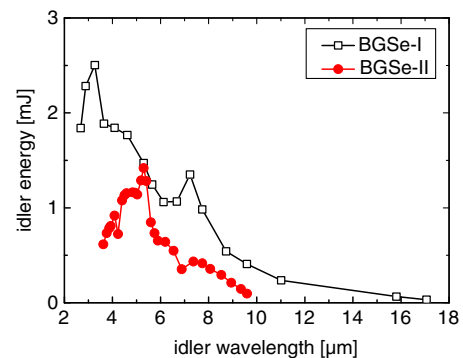


Fig. 4. Output idler energy versus wavelength for BGSe-I and BGSe-II. The cavity length is 32 mm, and the pump energy is 27 mJ.

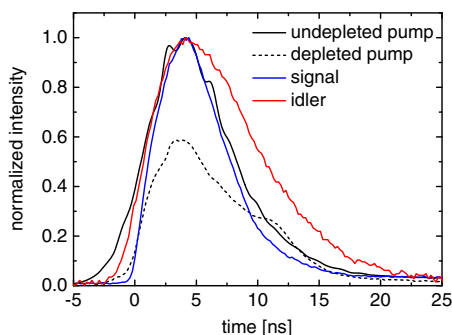


Fig. 5. Simultaneously measured temporal pulse shapes of the undepleted and depleted (by 38%) pump, signal, and idler for BGSe-II at normal incidence at a pump energy of 31.5 mJ.

observed for both crystals at normal incidence (7.2 and 5.3 μm , respectively) where additional feedback is provided by the Fresnel reflections. For BGSe-I, the idler energy increases to shorter wavelengths due to the increasing parametric gain; however, at some point, this trend is canceled by the increasing reflectivity of the ZnSe IOC for the idler. At longer wavelengths, the contributing factors besides the parametric gain are the BGSe crystal absorption (Fig. 1) and the IOC transmission. The performance of BGSe-II is similar, but here the idler energy starts to drop at shorter wavelengths much closer to the point corresponding to normal incidence, in accordance with the IOC characteristics. Some additional features might be related to air absorption. Still, the data in Fig. 4 seem to support the conclusions about the nonlinear coefficient d_{16} made before.

The OPO linewidth for the signal wave was measured at normal incidence using a 1 mm thick Ag-coated CaF_2 Fabry-Perot etalon: it was ~ 40 GHz both for BGSe-I and BGSe-II. Convolution of this value with the spectral extent of the pump (30 GHz), assuming Gaussian shapes, gives a spectral FWHM of 9 nm at 7.2 μm (BGSe-I) and 5 nm at 5.3 μm (BGSe-II).

Figure 5 shows the temporal characteristics of the pulses measured for BGSe-II using a fast InGaAs photodiode (pump and signal) or a (HgCdZn)Te detector (Vigo systems model PCI-9, Poland) with a time constant of < 2 ns (idler), connected to a 2 GHz oscilloscope. As a result of depletion and back-conversion, the pump pulse is reshaped and lengthened at high conversion efficiencies. The ~ 10 ns FWHM of the idler at 5.3 μm can be considered as an upper limit at a high conversion efficiency due to the limited temporal resolution. Very similar results were obtained with BGSe-I at 7.2 μm . Thus, the output pulse durations are rather close to that of the pump which means short buildup time, resulting in a high conversion efficiency. At lower pump levels, they are somewhat shorter, ~ 6 ns (signal) and ~ 8 ns (idler).

The idler beam spatial profiles were recorded by a SpiriconTMPyrocam III camera equipped with LiTaO_3 pyroelectric detector (active area, 12.4×12.4 mm; element size, 0.1×0.1 mm). The ISO standardized second-moment σ beam width ($D_{4\sigma} = 4\sigma$) was selected as an evaluation method because, as could be expected for the nonresonated wave at a high conversion efficiency, the idler beam shape is far from Gaussian, showing typical for back-conversion distortions such as donut shapes. At a pump level of 31.5 mJ and normal incidence, the M^2 values obtained for the idler were between 40 and 60 in the two planes, both for BGSe-I and BGSe-II. Other factors that

contribute to these high values, besides the high conversion efficiency far above threshold, are the large Fresnel number and the short pump pulse duration. Obviously, as with HGS, one could improve this situation by employing a RISTRA cavity [16]. The possibility to operate both type-I and type-II BGSe at the same idler wavelength with similar efficiency offers a good option to compare the role of spatial walk-off effects for the RISTRA concept when the idler is e- or o-polarized.

In conclusion, the newly developed monoclinic chalcogenide crystal BGSe showed excellent optical quality and performance in a 1.064 μm pumped nanosecond OPO. It generated the highest pulse energy for a non-oxide crystal in such an OPO above the 5 μm limit of oxide materials. Unprecedented tuning capability from 2.7 to 17 μm could be achieved with a single crystal cut. Pump-to-idler conversion efficiencies exceed previously reported values by a factor of ~ 3 , whereas the pump depletion reached 40%.

Both type-I and II phase matching are very efficient for frequency downconversion. Explanation of the results requires further efforts to determine the magnitude and sign of the non-diagonal second-order susceptibility tensor elements.

Future experiments will be devoted to operation at higher repetition rates [11] and implementation of the RISTRA concept for improvement of the spatial beam quality.

Funding. Deutscher Akademischer Austauschdienst (DAAD) Michail-Lomonosov-Programme-Linie A (2014, 2015) (50015386, 57180771); Ministry of Education and Science of the Russian Federation (NSU project 5-100).

REFERENCES

- V. Petrov, Prog. Quantum Electron. **42**, 1 (2015).
- V. Petrov, IEEE J. Sel. Top. Quantum Electron. **21**, 1602914 (2015).
- K. L. Vodopyanov, J. P. Maffettone, I. Zwieback, and W. Ruderman, Appl. Phys. Lett. **75**, 1204 (1999).
- A. Esteban-Martin, G. Marchev, V. Badikov, V. Panyutin, V. Petrov, G. Shevyrdyaeva, D. Badikov, M. Starikova, S. Sheina, A. Fintisova, and A. Tyazhev, Laser Photon. Rev. **7**, L89 (2013).
- A. Tyazhev, D. Kolker, G. Marchev, V. Badikov, D. Badikov, G. Shevyrdyaeva, V. Panyutin, and V. Petrov, Opt. Lett. **37**, 4146 (2012).
- J. Yao, D. Mei, L. Bai, Z. Lin, W. Yin, P. Fu, and Y. Wu, Inorg. Chem. **49**, 9212 (2010).
- V. Badikov, D. Badikov, G. Shevyrdyaeva, A. Tyazhev, G. Marchev, V. Panyutin, V. Petrov, and A. Kwasniewski, Phys. Status Solidi **5**, 31 (2011).
- J. Yao, W. Yin, K. Feng, X. Li, D. Mei, Q. Lu, Y. Ni, Z. Zhang, Z. Hu, and Y. Wu, J. Cryst. Growth **346**, 1 (2012).
- F. Yang, J. Yao, H. Xu, K. Feng, W. Yin, F. Li, J. Yang, S. Du, Q. Peng, J. Zhang, D. Cui, Y. Wu, C. Chen, and Z. Xu, Opt. Lett. **38**, 3903 (2013).
- F. Yang, J.-Y. Yao, H.-Y. Xu, F.-F. Zhang, N.-X. Zhai, Z.-H. Lin, N. Zong, Q.-J. Peng, J.-Y. Zhang, D.-F. Cui, Y.-C. Wu, C.-T. Chen, and Z.-Y. Xu, IEEE Photon. Technol. Lett. **27**, 1100 (2015).
- J.-H. Yuan, C. Li, B.-Q. Yao, J.-Y. Yao, X.-M. Duan, Y.-Y. Li, Y.-J. Shen, Y.-C. Wu, Z. Cui, and T.-Y. Dai, Opt. Express **24**, 6083 (2016).
- E. Boursier, P. Segonds, J. Debray, P. L. Inácio, V. Panyutin, V. Badikov, D. Badikov, V. Petrov, and B. Boulanger, Opt. Lett. **40**, 4591 (2015).
- P. Tzankov and V. Petrov, Appl. Opt. **44**, 6971 (2005).
- X. Zhang, J. Yao, W. Yin, Y. Zhu, Y. Wu, and C. Chen, Opt. Express **23**, 552 (2015).
- E. Boursier, P. Segonds, B. Menaert, V. Badikov, V. Panyutin, D. Badikov, V. Petrov, and B. Boulanger, Opt. Lett. **41**, 2731 (2016).
- G. Marchev, M. Reza, V. Badikov, A. Esteban-Martin, G. Stöppler, M. Starikova, D. Badikov, V. Panyutin, M. Eichhorn, G. Shevyrdyaeva, A. Tyazhev, S. Sheina, A. Agnesi, A. Fintisova, and V. Petrov, Appl. Opt. **53**, 7951 (2014).